Diversity, Pathogenicity, and Biological Characteristics of Root Rot Pathogens from *Lycium barbarum* L.

Yongbao Zhao , Lingshan Wang , Kaifu Zheng , Chengwen Zheng , Lijie Liu , Hexing Qi *

Posted Date: 29 September 2025

doi: 10.20944/preprints202509.2297.v1

Keywords: Gouqi; root rot; *Fusarium* fungi; diversity; pathogenicity; biological characteristics

 doi:10.20944/preprints202509.2297.v1

Article

Diversity, Pathogenicity, and Biological Characteristics of Root Rot Pathogens from *Lycium barbarum* L.

Yongbao Zhao [1], Lingshan Wang [1], Kaifu Zheng [2], Chengwen Zheng [2], Lijie Liu [1] and Hexing Qi [1,*]

[1] College of Agriculture and Animal Husbandry, Qinghai University, Qinghai, Xining, 810016
[2] Qinghai University, Qinghai, Xining, 810016
* Correspondence: author. E-mail: qhx390495559@126.com. Tel: 86971-5318437

Abstract

***Lycium** barbarum* L. is an important economic crop in Qinghai province, China. However, root rot seriously reduces the economic results of *L. barbarum*. Here, we collected the diseased *L. barbarum* roots from Nuomuhong Farm of Haixi Mongolian and Tibetan Autonomous Prefecture, Qinghai Province, China, to clarify the diversity, pathogenicity, and biological characteristics of its root rot pathogens. A total of 125 isolates were collected, and based on morphological characteristics and rDNA-ITS, *TEF-1α*, and *RPB2* gene sequence analysis, they were identified as *Fusarium equiseti*, *F. avenaceum*, *F. solani*, *F. citri*, *F. acuminatum*, *F. culmorum*, *F. sambucinum*, *F. incarnatum*, *F. oxysporum*, *F. tricinctum*, *Microdochium bolleyi*, and *Clonostachys rosea*. These fungi were used to inoculate the roots of 1-year-old *L. barbarum* seedlings using scratching and root-irrigation inoculation methods, and all isolates caused root rot. The lethal temperatures were 50°C for *F. acuminatum*, *F. sambucinum*, and *F. culmorum*; 55°C for *F. equiseti, C. rosea, M. bolleyi, F. avenaceum, F. citri, F. incarnatum, and F. tricinctum*; and 65°C for *F. solani, and F. oxysporum*. The best media for the 12 pathogen species were potato dextrose agar, mung bean soup culture, and carnation leaf piece agar. The optimum carbon sources were sucrose, dextrin, and soluble starch, and the optimum nitrogen sources were beef extract, peptone, and yeast extract. This is the first report that *M. bolleyi*, *F. avenaceum*, and *F. citri* cause root rot in *L. barbarum*. Moreover, our findings provide a theoretical foundation for root rot management in the future.

Keywords: Gouqi; root rot; *Fusarium* fungi; diversity; pathogenicity; biological characteristics

1. Introduction

"Gouqi" is the common name for *Lycium barbarum* L., which belongs to the Solanaceae family is a medicinal plant with a long history of use in traditional Chinese medicine [1]. The *Lycium* genus comprises approximately 70 species that vegetate in separate and distinct regions distributed from the temperate to the subtropical regions of Eurasia, North America, South America, southern Africa, and Australia [2]. In China, there are seven species and two varieties of the genus *Lycium*, four of which have been used by different ethnic groups. Only *L. barbarum* and *L. chinense* have been transformed into globally traded commodities. *Lycium barbarum* berries are red or orange-yellow and oblong or ovoid [3], and the morphological characteristics of *L. chinense* are similar to those of *L. barbarum*. The term Chinese-cultivated Gougi generally refers to *L. barbarum*, which has a long history of traditional use. In Northern and Central China, it has been used in traditional medicine for 2000 years to promote longevity, vision, and wellness. Since the Tang Dynasty, *L. barbarum* has been noted for its traditional health benefits, such as nourishing the yin, strengthening the liver and kidney, and

 doi:10.20944/preprints202509.2297.v1

sustaining the blood [4,5]. Modern studies have found that *L. barbarum* also has anti-aging, immunomodulation, anti-cancer, and anti-fatigue. Traditional Chinese medicine makes use of both the root bark (Digupi) and fruit (Gouqizi), moreover, fruit is well known in traditional Chinese herbal medicine and has been widely used as a popular functional food [6]. The utilization of its leaves and seeds has also been mentioned in a few medicinal books [7]. The nutritional effects of *L. barbarum* are mainly due to its rich content of compounds such as polysaccharides, flavonoid polyphenols, carotenoids, and alkaloids [8,9]. Therefore, the demand for Gouqi and its price are increasing in China.

Fusarium species, which are part of the Nectriaceae family in the Hypocreales order within the Ascomycota phylum, are widely distributed across environments such as air, water, soil, plants, insects, and organic substrates. This genus encompasses over 200 species grouped into 22 species complexes [10]. The name *Fusarium* was coined by Fries in 1821, and its species are recognized as one of the most important pathogens in agriculture and horticulture, infecting a variety of crops [11]. In addition, this genus of pathogenic fungi is known in the food industry [12]. *Fusarium* species are major soil-borne pathogens. In China, they are common in the northwest, southwest, central, and southeast regions. They cause economic losses by limiting crop growth and yield and pose a threat to food safety and human health by producing fungal toxins, such as trichothecene, fumonisins, and zearalenone [13–16]. Of the top 10 pathogenic fungi in molecular plant pathology in 2012, *F. graminearum* and *F. oxysporum* ranked fourth and fifth, respectively, indicating that *Fusarium* fungi have a strong destructive effect as plant pathogens [17]. *Fusarium* species cause many diseases. For example, *F. graminearum* and *F. verticillioides* cause ear rot in *Zea mays*; *Fusarium solani* causes collar rot in *Pisum sativum* [18]. *Fusarium oxysporum* causes Fusarium wilt in banana, having a serious impact on banana production worldwide [19]. *Fusarium graminearum* causes Fusarium head blight on *Triticum aestivum* [20]. *Fusarium fujikuroi* causes rice bakanae disease [21], and *F. graminearum* causes *Z. mays* stalk rot [22]. Moreover, *Fusarium* species interact with other plant pathogens, and mycotoxin accumulation plays an important role in disease outbreaks [23].

Microdochium bolleyi typically resides endophytically in plant roots, especially in herbaceous plants, and is abundant in the roots of coastal herbaceous plant species along the Pacific Northwest coast of the United States [24]. *Microdochium bolleyi* primarily colonizing the roots of cereals and grasses, including *T. aestivum* and *Hordeum vulgare*, suppresses some plant pathogens affecting cereals. The formation of typical chlamydospore clusters, which are visible under light microscopy, in colonized plant cells makes this endophytic fungus an excellent model organism for studying plant–endophyte interactions [25]. However, some studies have shown that *M. bolleyi* causes crown and root rot in grasses, such as *T. aestivum* and *H. vulgare* [26], and is associated with basal rot of *Agrostis stolonifera* [27] and root rot in *Linum usitatissimum* [28]. Therefore, *M. bolleyi* is generally considered a commensal or weak pathogen [24].

Clonostachys rosea is a filamentous fungus with a widespread distribution across a range of habitats [29]. *Clonostachys rosea* is a potent biocontrol agent against *F. oxysporum*, using mycoparasitism and its bioactive metabolites [30], and reduces the severity of diseases caused by soil- and seed-borne pathogens [31]. However, *C. rosea* can also cause root rot and was first reported on *Glycine max* in the United States [32]. It can also cause stem end rot of *Actinidia chinensis* [32] and root rot of naked *H. vulgare* var. *nudum*, *Xanthoceras sorbifolium* [34], *G. max* [35], *Allium sativum* [36], and *Astragalus membranaceus* [37].

Root rot is one of the most common diseases affecting *L. barbarum*, seriously affecting its quality and posing a huge threat to local economic development. In the early stages of the disease, the roots swell, intensifying in the middle stage with a small amount of defoliation. In the later stage, the roots rot and show reddish brown and the plants shed many leaves until they wither and die. In the main *L. barbarum* cultivation areas, the root rot incidence can reach 50%, resulting in serious yield and income reduction, hindering the development of the *L. barbarum* industry [38]. *Fusarium* species have been reported as the main pathogens causing root rot in *L. barbarum* [39]. Our investigation into root rot of *L. barbarum* in Qinghai Province from 2022 to 2023 revealed that root rot caused by *Fusarium*

 doi:10.20944/preprints202509.2297.v1

commonly occurred. The objectives of this study were to determine the phylogenetic diversity, morphological characteristics, and pathogenicity of isolates to *L. barbarum* and to clarify their biological characteristics to provide a foundation for comprehensive disease control.

2. Materials and Methods

2.1. Collection Site

Gouqi root rot samples were collected from Nuomuhong Farm (96° 14′ 59.95″–96° 30′ 37.46″ E, 36° 24′ 20.21″–36° 26′ 45.66″ N), Dulan County, Haixi Mongolian and Tibetan Autonomous Prefecture, Qinghai Province, China, at an altitude of 2800 m. The area covers 130,000 acres, with a low annual rainfall of 43.5 mm, strong solar radiation, and more than 3100 h of sunshine per year. The average annual temperature is 4.9°C, with distinct differences between day and night, and the annual maximum and minimum temperatures are 35.8 and −31°C, respectively. The frost-free period is 70 days [40]. The soil type is gray-brown desert soil and sandy soil, which is highly suitable for Gouqi growth. On the farm, the Gouqi planting area is approximately 80,000 acres, which is the largest Gouqi planting area in Qinghai Province. In this study, 36 samples showing root rot were collected in July and August 2022 and 2023 from 12 sites on the farm.

2.2. Media Used in the Study

Potato dextrose agar (PDA) [24] (200 g of potato, 20 g of glucose, 18 g of agar, and distilled water to a volume of 1000 mL) was used to preserve, activate, and observe the morphological characteristics of fungi. For isolations, 2% water agar (2% WA) medium (20 g of agar and distilled water to a volume of 1000 mL) was used. The following media were used to evaluate the biological characteristics: carrot agar (CA) medium (200 g of carrot, 20 g of glucose, 20 g of agar, and distilled water to a volume of 1000 mL), carnation leaf-piece agar (CLA) medium (14.4 g of agar, distilled water to a volume of 1000 mL, and carnation leaves), complete (CM) medium (6 g of yeast extract, 3 g of enzymatic casein, 3 g of acid-hydrolyzed casein, 10 g of sucrose, 900 μL of dd H_2O, and distilled water to a volume of 1000 mL), mung bean soup culture (MB) medium (20 g of mung beans and distilled water to a volume of 1000 mL), and Czapek (Czapek–Dox) medium (3 g of sodium nitrate, 1 g of dipotassium hydrogen phosphate, 0.5 g of magnesium sulfate, 0.5 g of potassium chloride, 0.01 g of ferrous sulfate, 30 g of sucrose, 20 g of agar, and distilled water to 1000 mL).

2.3. Isolation, Purification, and Preservation of Pathogenic Fungi

To isolate the fungi, root pieces (approximately 0.5 cm) were obtained with sterile scissors from the junction of infected and healthy tissues. They were surface-disinfected with 3% NaClO for 1.5 min and washed 3 times with sterile water. The disinfected pieces were dried and placed on 2% WA plates in an incubator at 25°C for 2 days. After the root surface became moldy, abundant conidiophores and conidia formed. Conidia were placed into sterile water with a pipette to prepare a spore suspension. Then, 200 μL of the spore suspension was spread on the surface of a 2% WA plate and placed in an incubator at 25°C for 12 h. Single spores were selected under a stereomicroscope and cultured on PDA. A total of 125 isolates were collected from rotted roots. Fungal isolates were cultured on PDA at 25°C, maintained on filter paper, and stored at −20°C for long-term conservation [41].

2.4. Pathogen Identification

2.4.1. Morphological Identification

Colony and conidia morphology were observed, and isolates were identified according to the *Fusarium* Laboratory Manual [42]. Representative single spore isolates were used to inoculate a PDA plate and cultured for 5 days, and a mycelial block with a diameter of 5 mm was placed on a PDA plate. After 7 days of culture in an incubator at 25°C, the diameter was measured using the cross method. Each isolate was tested three times. Conidia were used to make temporary slides, and

 doi:10.20944/preprints202509.2297.v1

conidial morphology was observed under a 40× optical microscope (OLYMPUS IX71, Olympus, Tokyo, Japan). To characterize conidial morphology, the length and width of at least 30 conidia per isolate were observed under a light microscope and measured with Image-Pro Plus version 6.0.0 software (Media Cybernetics, Silver Spring, MD, USA). The length of a conidium from apex to base was defined as the conidial length, and the widest part of each conidium was defined as the conidial width.

2.4.2. DNA Extraction, PCR, and Sequencing

Genomic DNA was extracted from vegetative mycelia using the cetyltrimethylammonium bromide protocol [43]. DNA amplification was performed for the DNA sequences of the nuclear ribosomal internal transcribed spacer (rDNA-ITS), the translation elongation factor 1-alpha (*TEF-1α*), and the RNA polymerase II gene (*RPB2*). The PCRs were performed in 25-μL mixtures with 1 μL of genomic DNA, 12.5 μL of 2× Taq PCR Master Mix (Biomed, Beijing, China), and 10 μM of each primer. The following PCR primers were used: rDNA-ITS amplification primers, ITS1 (5′-TCCGTAGGTGAACCTGCGG-3′) and ITS4 (5′-TCCTCCGCTTATTGATATGC-3′) [44,45]; *TEF*-1*α* gene amplification primers, EF-1 (5′-ATGGGTAAGGARGACAAGAC-3′), EF-2 (5′-GGARGTACCAGTSATCATGTT-3′) [46,47]; and *RPB2* gene amplification primers, RPB2-5F (5′-GAYGAYMGWGATCAYTTYGG-3′), RPB2-7CR (5′-CCCATRGCTTGYTTRCCCAT-3′) [48]. DNA sequencing was performed at Tsingke Biological Technology Company (Beijing, China).

2.4.3. Phylogenetic Analysis

The phylogenetic tree was constructed with reference to Swofford [49]. DNA sequences were aligned with an online version of MAFFT (https://mafft.cbrc.jp/alignment/software/), and the alignment was manually adjusted using MEGA version 6.0.6 (Tokyo Metropolitan University, Tokyo, Japan). Maximum parsimony trees were constructed using PAUP* version 4.0 alpha for all datasets, and they were generated by heuristic searches with *Alternaria alternata* (GenBank accession number CBS 130263), as a reference taxon and 1000 bootstrap replicates. The sequences of the 21 reference strains were downloaded from the NCBI database. The NCBI accession numbers of 125 pathogens were PV592419–PV592543 for the ITS sequences, PV567778–PV567888 for *TEF-1α*, and PV595151–PV595275 for *RPB2*.

2.5. Pathogenicity Assays

All isolates were cultured on PDA plates at 25°C for 5 days, and a pathogenicity test was performed by inoculating the roots of 1-year-old *L. barbarum* seedlings with conidial suspensions at a concentration of 1×10^6 per mL in 0.025% Tween 20. Two inoculation methods, scratching and root-irrigation inoculation, were used to determine the pathogenicity of isolates to *L. barbarum*. For the scratching inoculation method, the root epidermis was evenly pierced with a sterile inoculation needle, and a 10 μL conidial suspension was used to inoculate each wound. Inoculated roots were incubated in a humid and dark chamber at 25°C for 14 days. For the root-irrigation inoculation method, the *L. barbarum* root epidermis was pierced, and a 15 mL spore suspension was poured into each pot to irrigate the roots. Inoculated plants were incubated in a humid and dark chamber at 25°C for 24 h and moved to a greenhouse with a 12-h light/12-h dark photoperiod for 30 days. Sterile water was used as a control. The pathogenicity test was repeated three times for each isolate.

2.6. Biological Characteristics of Pathogens

2.6.1. Effects of Different Media

PDA, CA, CLA, CM, and CB media 50 were used to investigate their effects on mycelial growth. A 5-mm diameter mycelial plug was transferred to the center of each medium and incubated at 25°C in an incubator for 7 days. Each isolate was repeated three times.

 doi:10.20944/preprints202509.2297.v1

2.6.2. Effects of Temperature

To determine the effect of temperature on mycelial growth, 5-mm diameter mycelial plugs of the isolates were incubated at different temperatures (35, 40, 50, 55, 60, 65, and 70°C) for 10 min and incubated at 25°C in an incubator for 7 days. Each isolate was repeated three times.

2.6.3. Effects of pH

To determine the effect of pH on mycelial growth, PDA media were adjusted with 0.1 M HCl and 0.1 M NaOH to obtain pH values of 4.0, 5.0, 6.0, 7.0, 8.0, 9.0, 10.0, and 11.0 [50,51]. A 5-mm diameter plug was placed in the center of a PDA plate and incubated at 25°C in an incubator for 7 days. Each isolate was repeated three times.

2.6.4. Effects of Carbon and Nitrogen

Czapek–Dox medium was used as the basic medium to determine the utilization of nitrogen and carbon sources [50]. In the media, 20 g of sucrose was replaced with 20 g of soluble starch, maltose, glucose, dextrin, cellulose, mannitol, lactose, fructose, and xylose to determine the effects of different carbon sources on growth. Furthermore, 4 g of sodium nitrate was replaced with 4 g of beef extract, peptone, yeast extract, urea, potassium nitrate, ammonium nitrate, ammonium chloride, and sodium nitrate to determine the effects of different nitrogen sources on growth. A 5-mm diameter mycelial plug was transferred to the center of each carbon source medium and nitrogen source medium, and plates were incubated at 25°C in an incubator for 7 days. Each isolate was repeated three times.

2.7. Data Processing

Microsoft Excel worksheet was used for data integration, IBM Statistics SPSS 20.0 software was used for one-way ANOVA, and Duncan's multiple range test was used to test the significance of differences.

3. Results

3.1. Field Symptoms of Gouqi Root Rot and the Diversity of Pathogenic Fungi

The incidence of Gouqi root rot at Nuomuhong Farm, Dulan County, Haixi Mongolian and Tibetan Autonomous Prefecture, Qinghai Province, China, was serious, with an incidence rate of 10–50%. The leaves on the ground were yellow, and some of the Gouqi leaves fell off (Figure 1B). The epidermis near the roots fell off, and the branches and main stems turned white and dry. The main roots of the underground part were short, and the number of roots was reduced. The fibrous roots were short and thin, and main and fibrous roots were rotted (Figure 1C).

 doi:10.20944/preprints202509.2297.v1

Figure 1. Symptoms of root rot disease on *L. barbarum* in the field: A, healthy Gouqi; B, diseased Gouqi; and C, rotted roots of Gouqi.

A total of 125 pathogenic fungi were isolated from 36 root samples of cultivated Gouqi and identified using morphological and molecular biology techniques. There were 34 *F. equiseti*, 22 *C. rosea*, 14 *M. bolleyi*, 12 *F. solani*, 11 *F. acuminatum*, 8 *F. sambucinum*, 6 *F. avenaceum*, 6 *F. citri*, 5 *F. incarnatum*, 3 *F. culmorum*, 2 *F. oxysporum*, and 2 *F. tricinctum* isolates, with separation frequencies of 27.2, 17.6, 11.2, 9.6, 8.8, 6.4, 4.8, 4.8, 4.0, 2.4, 1.6, and 1.6%, respectively. Among them, *F. equiseti*, *C. rosea*, and *M. bolleyi* were the dominant pathogens, and *F. avenaceum*, *F. citri*, *F. incarnatum*, *F. culmorum*, *F. oxysporum*, and *F. tricinctum* were rare.

3.2. Morphology and Phylogenetic Analysis of Root Rot Pathogens

The morphological characteristics of the 125 pathogens were observed (Figure 2; Table 1). *Fusarium equiseti* colonized the whole plate in 7 d and produced pale yellow colony. Microconidia were sparse and measured 11.56 ± 1.46 × 3.85 ± 0.56 μm. Macroconidia were slightly curved with 1–5 septa and were 26.44 ± 2.14 × 5.69 ± 1.43 μm in size. Its chlamydospores were 16.34 ± 1.58 × 14.15 ± 2.08 μm in size.

 doi:10.20944/preprints202509.2297.v1

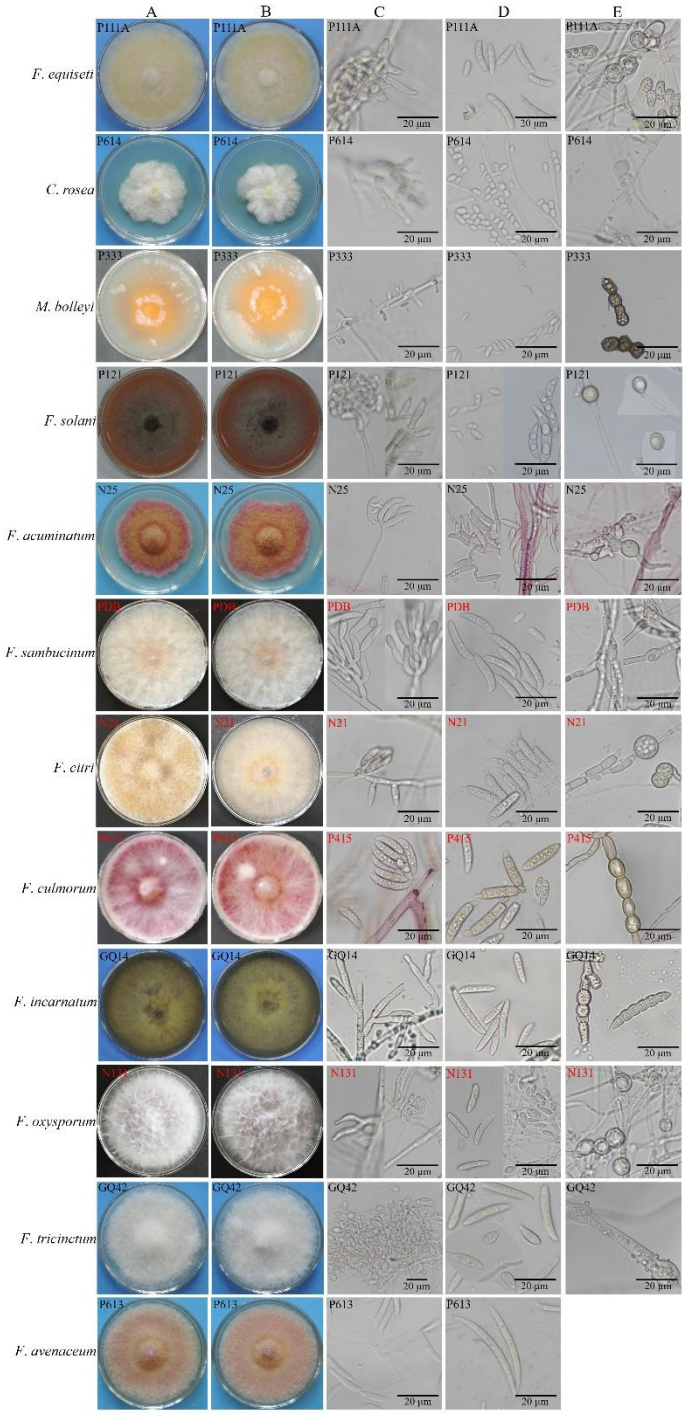

Figure 2. Morphological characteristics of root rot pathogens of Gouqi: A, colony morphology of original isolates; B, colony morphology of re-isolated isolates from infected roots after artificial inoculation; C, conidiophores; D, conidia; and E, chlamydospores.

Table 1. Conidia length and width of twelve species of root rot pathogens from *L. barbarum* (μm).

Types of spores	*F. equiseti*	*C. rosea*	*M. bolleyi*	*F. solani*	*F. acuminatum*	*F. sambucinum*	*F. avenaceum*	*F. citri*	*F. incarnatum*	*F. culmorum*	*F. oxysporum*	*F. tricinctum*
conidia	11.56 ±1.46	7.04± 0.41×	9.55± 2.04×	7.63± 0.91×	8.82± 1.65×	7.72± 1.36×	rare	rare	rare	8.24± 1.56×	7.22± 1.12×	13.20 ±2.16

 doi:10.20944/preprints202509.2297.v1

nidia	onidium	×3.85 ±0.56	4.36± 0.37	3.39± 0.78	4.7±0.68	4.32± 0.83	4.22± 0.92				4.43 ±1.14	3.26± 0.70	×4.52 ±1.44
	macroconidium	26.44 ±2.14 ×5.69 ±1.43			39.09 ±4.63 ×7.07 ±1.21	20.16 ±3.02 ×4.79 ±0.88	34.75 ±5.38 ×7.56 ±1.20	46.45±4.96× 5.74 ±1.54	30.84 ±5.41 ×5.72 ±1.02	30.02 ±1.51 ×6.17 ±1.07	37.99 ±1.96 ×8.97 ±0.46	33.68 ±2.21 ×11.4 5±0.42	33.97 ±4.95 ×7.17 ±1.34
	chlamydospore	16.34 ±1.58 ×14.15±2.08	11.38 ±2.25 ×12.45±2.02	11.28 ±1.46 ×8.00 ±0.59	15.74 ±2.02 ×14.19±1.90	13.07 ±2.15 ×12.84±1.23	13.12 ±3.80 × 9.45± 2.15	not found	11.32 ±2.10 ×10.57±2.93	13.06 ±3.48 ×16.73±2.54	13.77 ±2.71 ×11.91±1.79	13.91 ±1.36 ×12.77±1.68	14.76 ±4.45 ×13.56±2.25

Clonostachys rosea formed a white mold, the hypha was colorless with septa, and conidiophores were broom-shaped. Conidia colorless, round or oval, no septum, 7.04 ± 0.41 × 4.36 ± 0.37 μm in size, and chlamydospores were 11.38 ± 2.25 × 12.45 ± 2.02 μm in size.

Microdochium bolleyi produced few aerial mycelia, and the middle of the colony was orange. It produced a large number of conidia that were colorless and slightly curved. Conidia were produced laterally on the conidiophore, about 9.55 ± 2.04 × 3.39 ± 0.78 μm in size, and chlamydospores were 11.28 ± 1.46 × 8.00 ± 0.59 μm in size.

The aerial mycelium of *F. solani* had weak growth, producing less mycelia. The mycelia were white in the early stage and produced red, purple, or blue pigments in the later growth stage. It produced many macroconidia and microconidia. Macroconidia were colorless, with 1–4 septa, and were 39.09 ± 4.63 × 7.07 ± 1.21 μm in size. Microconidia were ovate to round and single-spored, with a size of 7.63 ± 0.91 × 4.7 ± 0.68 μm. Chlamydospores were round or oval, with a size of 15.74 ± 2.02 × 14.19 ± 1.90 μm.

Fusarium acuminatum produced abundant, dense aerial hypha that was rose red and had a slow growth rate. Macroconidia were colorless and falciform, had 1–3 septa, and were 20.16 ± 3.02 × 4.79 ± 0.88 μm in size. Microconidia were hyaline, had 0–1 septa, and were 8.82 ± 1.65 × 4.32 ± 0.83 μm in size. Chlamydospores were 13.07 ± 2.15 × 12.84 ± 1.23 μm in size.

The mycelia of *F. sambucinum* were loose, covered the dish in 7 days, and was light orange near the center. Macroconidia were fascicled, had 1–4 septa, and were 34.75 ± 5.38 × 7.56 ± 1.20 μm in size. Microconidia were colorless, had 0–1 septa, and were 7.72 ± 1.36 × 4.22 ± 0.92 μm in size. Chlamydospores were 13.12 ± 3.80 × 9.45 ± 2.15 μm in size.

The aerial hyphae of *F. avenaceum* were villous and pale red, and macroconidia were thin at both ends and wide in the middle, 46.45 ± 4.96 × 5.74 ± 1.54 μm in size, and had 1–7 septa. Conidiogenous cells arose laterally, and were phialidic and slender. Chlamydospores were not found.

Fusarium citri grew abundant, dense pale-yellow mycelia. Its macroconidia were colorless and laterally on conidiophores, with 1–5 septa. The tip of macroconidia was curved, and they were 30.84 ± 5.41 × 5.72 ± 1.02 μm in size. Microconidia were rare. Chlamydospores were round or oval and were 11.32 ± 2.10 × 10.57 ± 2.93 μm in size.

Fusarium incarnatum grew fast and had dense hyphae, and the surface was dark yellow. Macroconidia were colorless and 30.02 ± 1.51 × 6.17 ± 1.07 μm in size and had 1–5 septa. Microconidia were rare. Chlamydospores were 13.06 ± 3.48 × 16.73 ± 2.54 μm in size.

The aerial hypha of *F. culmorum* was sparse, and the colony was red. The top and bottom sides of the colony were initially dark red in the middle, surrounded by light red, and the dish was covered

 doi:10.20944/preprints202509.2297.v1

after 7 days. Macroconidia were pale yellow or colorless, with 1–4 septa, and were 37.99 ± 1.96 × 8.97 ± 0.46 μm in size. Microconidia were colorless, ovoid, and 8.24 ± 1.56 × 4.43 ± 1.14 μm in size and had 0–2 septa. Chlamydospores were round or ovoid and 13.77 ± 2.71 × 11.91 ± 1.79 μm in size.

The aerial hyphae of *F. oxysporum* were panniform and grew fast. The colony was light purple in the middle. Microconidia were rich, colorless, 7.22 ± 1.12 × 3.26 ± 0.70 μm in size, and had 0–1 septum. Macroconidia were colorless, 33.68 ± 2.21 × 11.45 ± 0.42 μm in size, and had 1–4 septa. Chlamydospores were 13.91 ± 1.36 × 12.77 ± 1.68 μm in size.

Fusarium tricinctum had white flocculent mycelia that covered the dish in 7 d. Its macroconidia were colorless, falciform, and slightly curved, with 1–5 septa, and were 33.97 ± 4.95 × 7.17 ± 1.34 μm in size. Microconidia were limoniform, oval, or pyriform, with 0–1 septa, and were 13.20 ± 2.16 × 4.52 ± 1.44 μm in size. Chlamydospores were 14.76 ± 6.45 × 13.56 ± 2.25 μm in size.

Values are presented as the mean ± standard deviatioThe single most parsimonious trees were generated from the combined sequences of rDNA-ITS and *RPB2* genes (Figure 3), as the *TEF-1α* gene of *M. bolleyi* was not amplified using the primers used in this study, and individual rDNA-ITS, *TEF-1α, and RPB2* genes from 125 isolates (Figures S1–S3). A total of 22 strains published in the NCBI database were used as reference strains (gray characters in Figures 3 and S1–S3). Overall, the trees in each phylogeny had the same topology, and 11 or 12 clades with high bootstrap values were resolved in the phylogenies inferred for *F. equiseti*, *C. rosea*, *M. Bolleyi*, *F. solani*, *F. acuminatum*, *F. sambucinum*, *F. avenaceum*, *F. citri*, *F. incarnatum*, *F. culmorum*, *F. oxysporum*, and *F. tricinctum*. In total, 22 isolates and 2 control strains (SJ123 and SJ62) clustered in the *C. rosea* clade, and 11 isolates and 2 control strains (NRRL5 4212 and NRRL 54214) clustered in the F. *acuminatum* clade. P612A, P415, P612B, and P111 clustered in the *F. culmorum* clade; N131 and GQ421 in the *F. oxysporum* clade; and GQ42 with control isolates CBS 110262, CBS133023, and CBS 25350 in the *F. tricinctum* clade. Five isolates and two control strains (CBS 132194 and CBS 133024) clustered in the *F. incarnatum* clade, and six isolates and two control strains (CBS 12173 and NRRL 54939) clustered in the *F. avenaceum* clade. Five isolates and two control strains (CBS 130905 and NRRL 25084) clustered in the *F. citri* clade, and nine isolates and two control strains (CBS 14695 and QJ 20911) clustered in the *F. sambucinum* clade. Thirty-four isolates and two control strain (CBS 18534 and CBS 30794) clustered in the *F. equiseti* clade. Twelve isolates and two control strains (CBS 102429 and CBS 131775) clustered in the *F. solani* clade. Fourteen isolates and two control strains (CBS 54092 and KAS 1350) clustered in the *M. bolleyi* clade.

 doi:10.20944/preprints202509.2297.v1

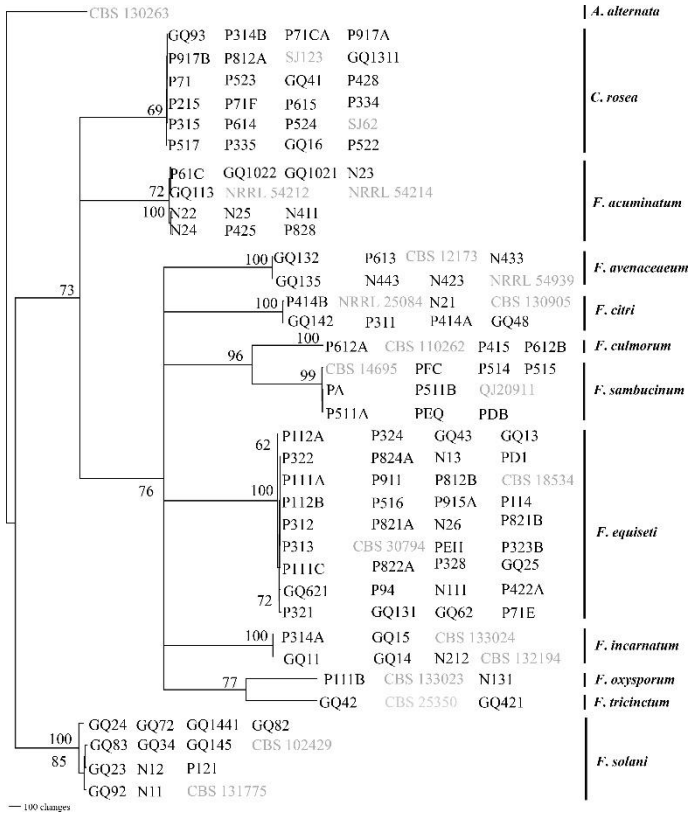

Figure 3. Maximum parsimony tree of root rot pathogens from Gouqi inferred from combined rDNA-ITS, *EF-1α*, and RPB2 sequences. The tree length is 14355. The consistency index (CI), retention index (RI), and rescaled consistency (RC) index were 0.531, 0.939, and 0.498, respectively.

3.3. Pathogenicity Analysis

The pathogenicity test was conducted using scratching and root-irrigation inoculation methods. The results of scratching inoculation showed that all isolates caused root rot in *L. barbarum* (Figure 4). Notably, distinct black lesions were observed after inoculation with *F. solani*, *F. avenaceum*, and *F. citri*. In contrast, the control group displayed lighter coloration with no symptoms. Robust mycelial growth was visible, with discoloration and decay around the wound, following inoculation with *F. tricinctum*, *F. oxysporum*, and *C. rosea*. Inoculation with *F. oxysporum*, *F. equiseti*, and *F. sambucinum* resulted in significant root decay and a color change at the inoculation site, confirming the disease. Inoculation with *M. bolleyi* and *F. culmorum* led to color changes and rot at the inoculation site.

Figure 4. Root rot symptoms of Gouqi using the scratching inoculation method.

The results of root-irrigation inoculation showed that all isolates could cause root rot. Thirty days after inoculation, the plants exhibited stunted growth and wilting and drying symptoms (Figure

 doi:10.20944/preprints202509.2297.v1

5A and B). Root rot was evident, with internal discoloration visible upon cutting, and black lesions appeared centrally. In contrast, the blank control roots showed no decay or discoloration, maintaining a milky white appearance. Inoculation with *F. solani*, *F. oxysporum*, *F. sambucinum*, and *F. avenaceum* resulted in pronounced internal root discoloration, with the blackened areas larger than those observed after inoculation with other pathogens (Figure 5C and D). Pathogens were re-isolated from the diseased roots, and their morphology matched that of the field pathogens (Figure 2A and B).

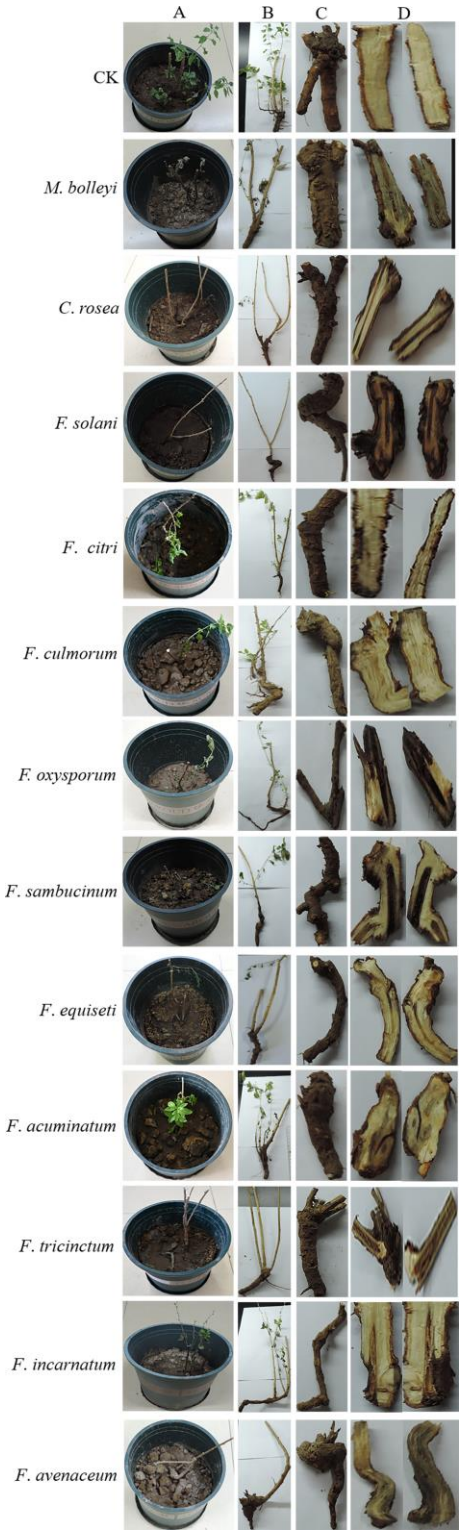

Figure 5. Root rot symptoms of Gouqi using the root-irrigation inoculation method. A, aboveground part; B, inoculated seedlings; C, underground part; and D, root cross-section.

 doi:10.20944/preprints202509.2297.v1

3.4. Biological Characteristics of Root Rot Pathogens

3.4.1. Effect of Different Media on Mycelial Growth

The optimum culture medium for the 12 pathogen species was determined using PDA, CM, MB, CLA, and CA media. The results showed that the best media were PDA, MB, and CLA. The optimum culture medium for *F. solani*, *F. sambucinum*, *F. avenaceum*, *F. citri*, *F. incarnatum*, *F. culmorum*, *and F. oxysporum* was PDA, with growth rates ranging from 0.78 to 0.80 mm/d. The optimum culture medium for *F. equiseti*, *C. rosea*, *F. culmorum*, *F. oxysporum*, *and F. citri* was MB, with growth rates ranging from 0.61 to 0.80 mm/d. The optimum culture medium for *F. culmorum*, *F. oxysporum*, *F. tricinctum*, *M. bolleyi*, *F. acuminatum*, and *F. citri* was CLA, with growth rates ranging from 0.69 to 0.80 mm/d. *Fusarium equiseti*, *C. rosea*, and *Fusarium acuminatum* had the worst growth on PDA, with growth rates of 0.68 ± 0.06, 0.44 ± 0.04, and 0.52±0.01 mm/d, respectively. *Microdochium bolleyi* showed the worst growth on CA, with growth rates of 0.28 ± 0.02. MB resulted in the worst growth for *F. avenaceum*, with growth rates of 0.56±0.06 mm/d. (Table 2, Figure S4).

Table 2. Effects of different media on the growth rate of root rot pathogens from *L. barbarum* (mm).

Media	*F. equiseti*	*C. rosea*	*M. bolleyi*	*F. solani*	*F. acuminatum*	*F. sambucinum*	*F. avenaceum*	*F. citri*	*F. incarnatum*	*F. culmorum*	*F. oxysporum*	*F. tricinctum*
PDA	0.68±0.06b	0.44±0.04b	0.47±0.19bc	0.78±0.01a	0.52±0.01c	0.80±0.00a	0.80±0.01a	0.80±0.00ab	0.80±0.00a	0.80±0.0 0a	0.80±0.00a	0.72±0.08ab
CM	0.79±0.00a	0.50±0.01b	0.34±0.02c	0.77±0.01b	0.52±0.06c	0.80±0.01a	0.62±0.07b	0.80±0.01a	0.80±0.01a	0.80±0.0 0a	0.78±0.01c	0.64±0.09bc
CA	0.79±0.00a	0.50±0.07b	0.28±0.02c	0.72±0.01d	0.62±0.07b	0.80±0.00a	0.77±0.03a	0.79±0.01b	0.80±0.00a	0.80±0.0 0a	0.79±0.01b	0.68±0.07bc
MB	0.80±0.01a	0.61±0.04a	0.60±0.16ab	0.76±0.01b	0.53±0.01c	0.76±0.04a	0.56±0.06c	0.80±0.00ab	0.81±0.01a	0.80±0.0 0a	0.80±0.01a	0.61±0.05c
CLA	0.79±0.01a	0.48±0.03b	0.69±0.03a	0.73±0.00c	0.74±0.03a	0.78±0.03a	0.79±0.01a	0.80±0.01a	0.79±0.02b	0.80±0.0 0a	0.80±0.00a	0.80±0.01a

Values are presented as the mean ± standard deviation. Letters represent the significance of differences.

3.4.2. Effect of Temperature on Mycelial Growth

The lethal temperatures of the 12 pathogen species were between 50 and 65°C. The lethal temperatures were 50°C for *F. acuminatum*, *F. sambucinum*, and *F. culmorum*; 55°C for *F. equiseti*, *C. rosea*, *M. bolleyi*, *F. avenaceum*, *F. citri*, *F. incarnatum*, and *F. tricinctum*; and 65°C for *F. solani*, and *F. oxysporum* (Table 3, Figure S5).

Table 3. Effects of different temperatures on the growth rate of pathogens from *L. barbarum* (mm).

Temperature	*F. equiseti*	*C. rosea*	*M. bolleyi*	*F. solani*	*F. acuminatum*	*F. sambucinum*	*F. avenaceum*	*F. citri*	*F. incarnatum*	*F. culmorum*	*F. oxysporum*	*F. tricinctum*
35°C	0.76±0.03a	0.51±0.05a	0.36±0.03a	0.77±0.01a	0.61±0.01a	0.79±0.01a	0.80±0.01a	0.79±0.01a	0.79±0.01a	0.80±0.01a	0.79±0a	0.79±0.01a
40°C	0.78±0.02a	0.51±0.01a	0.34±0.01a	0.78±0.01a	0.61±0.03a	0.79±0.01a	0.78±0.01a	0.80±0.01a	0.79±0.01a	0.79±0.01a	0.80±0.01a	0.76±0.04a
50°C	0.77±0.03a	0.40±0.03b	0.25±0.01b	0.77±0.01a	0	0	0.17±0b	0.58±0.12b	0.79±0.01a	0	0.80±0.01a	0.63±0.05b
55°C	0	0	0	0.47±0b	0	0	0	0	0	0	0.79±0.01a	0
60°C	0	0	0	0.35±0c	0	0	0	0	0	0	0.80±0.01a	0
65°C	0	0	0	0	0	0	0	0	0	0	0	0

 doi:10.20944/preprints202509.2297.v1

70℃	0	0	0	0	0	0	0	0	0	0	0	0

Values are presented as the mean ± standard deviation. Letters represent the significance of differences.

3.4.3. Effect of pH on Mycelial Growth

The optimum pH of the 12 pathogen species ranged from 4 to 11. The optimum pH of *C. rosea*, *F. citri*, *F. oxysporum*, *F. sambucinum*, *F. equiseti*, and *F. tricinctum* was 4–7, with growth rates ranging from 0.52 ± 0.02 to 0.80 ± 0.01 mm/d. The optimum pH of *F. incarnatum*, *F. culmorum*, *C. rosea*, *F. solani*, *F. citri*, *F. oxysporum*, *F. sambucinum*, *F. equiseti*, *F. tricinctum*, and *F. avenaceum* was 7–11, with growth rates from 0.53 ± 0.03 to 0.80 ± 0.01 mm/d. The optimum pH of *M. bolleyi* was 9, showing growth rates of 0.59 ± 0.02 mm/d. The optimum pH of *F. acuminatum* was 8, with a growth rate of 0.73 ± 0.04 mm/d (Table 4, Figure S6).

Table 4. Effects of different Ph on the growth rate of pathogens from *L. barbarum* (mm).

pH value	*F. equiseti*	*C. rosea*	*M. bolleyi*	*F. solani*	*F. acuminatum*	*F. sambucinum*	*F. avenaceum*	*F. citri*	*F. incarnatum*	*F. culmorum*	*F. oxysporum*	*F. tricinctum*
4	0.59±0.02f	0.50±0.03c	0.43±0.01b	0.68±0.01e	0.45±0.03d	0.79±0.01ab	0.52±0.01e	0.80±0.01a	0.78±0.01e	0.79±0.01ab	0.70±0.02c	0.67±0.04d
5	0.70±0.02cd	0.52±0.02abc	0.36±0.01cde	0.71±0.00c	0.57±0.01c	0.79±0.01ab	0.70±0.02cd	0.79±0.01ab	0.79±0.01cd	0.79±0.00b	0.79±0.00a	0.77±0.02abc
6	0.73±0.01abc	0.54±0.03ab	0.35±0.01e	0.73±0.00ab	0.63±0.03b	0.79±0.01ab	0.76±0.03b	0.79±0.01ab	0.79±0.01bc	0.79±0.00b	0.79±0.00a	0.78±0.01ab
7	0.75±0.01a	0.53±0.00ab	0.35±0.01de	0.70±0.00d	0.64±0.03b	0.79±0.00b	0.79±0.01ab	0.79±0.01ab	0.78±0.01de	0.79±0.00b	0.79±0.02a	0.79±0.01a
8	0.73±0.04ab	0.53±0.03ab	0.38±0.01c	0.72±0.01b	0.73±0.04a	0.80±0.01a	0.79±0.01ab	0.79±0.01ab	0.80±0.00a	0.79±0.00b	0.75±0.01b	0.78±0.01ab
9	0.73±0.02abc	0.54±0.02a	0.59±0.02a	0.73±0.00ab	0.58±0.02c	0.80±0.01a	0.76±0.03b	0.80±0.01a	0.80±0.00a	0.79±0.01ab	0.79±0.01a	0.78±0.01ab
10	0.66±0.03e	0.51±0.01bc	0.36±0.04cd	0.74±0.01a	0.59±0.03c	0.79±0.01ab	0.72±0.02c	0.79±0.00b	0.80±0.00a	0.80±0.01a	0.80±0.01a	0.74±0.05c
11	0.70±0.02bcd	0.52±0.01abc	0.36±0.02cde	0.73±0.00ab	0.58±0.02c	0.79±0.01ab	0.68±0.03d	0.79±0.00b	0.80±0.01ab	0.79±0.01ab	0.79±0.01a	0.75±0.02bc

Values are presented as the mean ± standard deviation. Letters represent the significance of differences.

3.4.4. Effect of Carbon and Nitrogen Sources on Mycelial Growth

The optimum carbon sources for the 12 pathogen species were screened using 10 carbon sources. The optimum carbon source for *F. equiseti*, *F. citri*, *F. incarnatum*, *F. culmorum*, and *F. oxysporum* was sucrose, with growth rates of all were 0.80 mm/d. The optimum carbon source for *C. rosea* was fructose, with growth rates of 0.57 ± 0.03 mm/d. Dextrin was the optimum carbon source for *F. incarnatum*, *F. culmorum*, *F. oxysporum*, and *F. tricinctum* with growth rates of all were 0.80 mm/d. The optimum carbon source for *F. acuminatum* was cellulose, showing a growth rate of 0.72 ± 0.03 mm/d. Soluble starch was the optimum carbon source for *F. avenaceum*, *F. incarnatum*, *F. culmorum*, and *F. oxysporum*, resulting in growth rates of 0.76 ± 0.0, 0.80±0.01, 0.80±0.01, and 0.80±0.01 mm/d, respectively. The growth rates of CK for *F. equiseti*, *F. incarnatum*, *F. culmorum*, and *F. oxysporum* were also fast, but the mycelia were only a thin layer and grew poorly. Glucose, lactose, cellulose, and xylose were not good carbon sources for any of the 12 pathogen species. For example, lactose as the carbon source resulted in the worst growth for *F. equiseti*, *F. acuminatum*, *F. citri* and *F. tricinctum*, with growth rates ranging from 0.39 ± 0.03 to 0.65 ± 0.03 mm/d (Table 5, Figure S7).

Table 5. Effects of different carbon sources on the growth rate of pathogens from *L. barbarum* (mm).

 doi:10.20944/preprints202509.2297.v1

Carbon source	*F. equiseti*	*C. rosea*	*M. bolleyi*	*F. solani*	*F. acuminatum*	*F. sambucinum*	*F. avenaceum*	*F. citri*	*F. incarnatum*	*F. culmorum*	*F. oxysporum*	*F. tricinctum*
CK	0.80±0.01ab	0.44±0.03cd	0.30±0.01c	0.78±0.01a	0.64±0.01b	0.75±0.02b	0.62±0.03cd	0.73±0.03bc	0.79±0.01ab	0.79±0.00a	0.79±0.01ab	0.65±0.02d
gluc ose	0.76±0.05b	0.43±0.02d	0.35±0.02b	0.79±0.01a	0.48±0.02d	0.72±0.06bc	0.59±0.03de	0.73±0.04bc	0.77±0.03b	0.80±0.00a	0.80±0.01a	0.74±0.03b
sucr ose	0.80±0.00ab	0.43±0.01cd	0.63±0.02a	0.79±0.00a	0.46±0.02d	0.79±0.01a	0.64±0.05cd	0.80±0.00a	0.80±0.00a	0.80±0.00a	0.80±0.01a	0.79±0.01a
man nitol	0.80±0.01ab	0.45±0.03cd	0.37±0.20c	0.80±0.01a	0.39±0.02e	0.75±0.01b	0.46±0.03g	0.79±0.00a	0.79±0.01ab	0.79±0.01a	0.80±0.01a	0.71±0.06c
dext rin	0.79±0.01ab	0.48±0.07bc	0.30±0.03c	0.74±0.01c	0.52±0.01c	0.80±0.01a	0.75±0.04a	0.79±0.01a	0.80±0.01a	0.80±0.01a	0.80±0.01a	0.80±0.00a
malt ose	0.70±0.05c	0.50±0.06b	0.29±0.02c	0.73±0.02c	0.66±0.05a	0.61±0.04d	0.69±0.02b	0.75±0.02bc	0.80±0.01a	0.79±0.01a	0.80±0.01a	0.72±0.02bc
solu ble starch	0.79±0.01ab	0.43±0.03d	0.30±0.03c	0.76±0.02b	0.69±0.03a	0.80±0.01a	0.76±0.04a	0.79±0.01a	0.80±0.01a	0.80±0.01a	0.80±0.01a	0.79±0.01a
lacto se	0.65±0.03d	0.44±0.08bcd	0.24±0.03de	0.73±0.01c	0.39±0.03e	0.71±0.01c	0.56±0.03ef	0.63±0.04d	0.64±0.02d	0.69±0.17b	0.78±0.01b	0.47±0.02f
cellu lose	0.79±0.01ab	0.51±0.04b	0.37±0.02b	0.79±0.01a	0.72±0.03a	0.79±0.01a	0.70±0.03b	0.79±0.00a	0.17±0.02e	0.79±0.00a	0.79±0.01ab	0.78±0.01a
fruct ose	0.79±0.01ab	0.57±0.03a	0.25±0.02de	0.79±0.00a	0.53±0.02c	0.79±0.00a	0.58±0.02def	0.79±0.00a	0.78±0.01ab	0.79±0.00a	0.80±0.01a	0.70±0.02c

 doi:10.20944/preprints202509.2297.v1

xylo se	0.72± 0.04c	0.44± 0.02c d	0.21± 0.03e	0.76 ±0.0 1b	0.46± 0.04d	0.74± 0.02b c	0.54± 0.02f	0.72± 0.01c	0.75± 0.02c	0.79± 0.01a	0.79± 0.01a b	0.59± 0.02e

Values are presented as the mean ± standard deviation. Letters represent the significance of differences.

The optimum nitrogen sources for the 12 pathogen species were determined using 8 nitrogen sources, and we found that beef extract, peptone, and yeast powder resulted in optimum growth. The optimum nitrogen source for *F. oxysporum*, *F. tricinctum*, *F. equiseti*, *M. bolleyi*, *F. sambucinum*, *F. incarnatum*, *and F. culmorum* was beef extract, showing growth rates of 0.80 mm/d. Peptone was the optimum nitrogen source for *F. equiseti*, *C. rosea*, *M. bolleyi*, *F. incarnatum*, *F. culmorum*, *F. oxysporum*, *F. tricinctum*. Yeast powder was the optimum nitrogen source for *F. equiseti*, *M. bolleyi*, *F. sambucinum*, *F. avenaceum*, *F. citri*, *F. incarnatum*, *F. culmorum*, *F. oxysporum*, *F. tricinctum*, and with growth rates ranging from 0.78 to 0.80 mm/d. Saltpeter was the optimum nitrogen source for *F. equiseti*, and *C. rosea*, with a growth rate of 0.80±0.01, and 0.51 ± 0.06 mm/d, respectively. The optimum nitrogen source for *F. solani* was sodium nitrate, with a growth rate of 0.79 ± 0.01 mm/d. The growth rates of CK for *F. equiseti*, *F. acuminatum*, *F. culmorum*, and *F. oxysporum* were fast, however, the mycelia were sparse and only a thin layer. The worst growth was observed on the media with ammonium chloride, and ammonium nitrate, respectively, with growth rates ranging from 0.28 ± 0.04 to 0.79 ± 0.00 mm/d (Table 6, Figure S8).

Table 6. Effects of different nitrogen sources on the growth rate of pathogens from *L. barbarum* (mm).

Nitrogen source	***F. equiseti***	***C. rosea***	***M. bolleyi***	***F. solani***	***F. acuminatum***	***F. sambucinum***	***F. avenaceum***	***F. citri***	***F. incarnatum***	***F. culmorum***	***F. oxysporum***	***F. tricinctum***
CK	0.80± 0.00a	0.44± 0.04bc	0.63± 0.02c	0.71± 0.02b	0.71±0 .05a	0.69±0 .03d	0.54± 0.02c	0.62± 0.08c	0.61± 0.04e	0.80±0 .01ab	0.74± 0.02c	0.73± 0.01b
beef extract	0.80± 0.00a	0.43± 0.01bc	0.80± 0.00a	0.76± 0.02a	0.57±0 .10cd	0.80±0 .00a	0.75± 0.03a	0.71± 0.00b	0.80± 0.00a	0.80±0 .00a	0.80± 0.00a	0.80± 0.01a
urea	0.80± 0.01a	0.38± 0.01cd	0.69± 0.01b	0.64± 0.01c	0.37±0 .01f	0.71±0 .02cd	0.49± 0.08d	0.68± 0.03b	0.72± 0.04c	0.80±0 .00a	0.79± 0.01ab	0.49± 0.02d
peptone	0.80± 0.00a	0.51± 0.10a	0.80± 0.00a	0.72± 0.02b	0.64±0 .05bc	0.74±0 .04bc	0.76± 0.02a	0.78± 0.04a	0.80± 0.00a	0.80±0 .00a	0.80± 0.01ab	0.80± 0.01a
yeast powder	0.80± 0.01a	0.45± 0.01ab	0.80± 0.00a	0.71± 0.01b	0.59±0 .06bc	0.80±0 .01a	0.78± 0.02a	0.80± 0.00a	0.80± 0.00a	0.80±0 .01ab	0.80± 0.00a	0.80± 0.00a

 doi:10.20944/preprints202509.2297.v1

sodium nitrate	0.79±0.01a	0.42±0.02bc	0.25±0.01f	0.79±0.01a	0.51±0.02d	0.77±0.02ab	0.69±0.04b	0.79±0.01a	0.78±0.01ab	0.80±0.00a	0.79±0.01ab	0.73±0.04b
ammonium chloride	0.64±0.05b	0.28±0.04e	0.59±0.05d	0.49±0.05e	0.35±0.05f	0.53±0.07e	0.34±0.04e	0.42±0.03d	0.50±0.04f	0.78±0.03c	0.67±0.03d	0.45±0.05e
ammonium nitrate	0.79±0.00a	0.35±0.03d	0.71±0.03b	0.60±0.02d	0.44±0.01e	0.78±0.01ab	0.48±0.04d	0.63±0.06c	0.65±0.02d	0.79±0.01abc	0.78±0.01b	0.65±0.03c
saltpeter	0.80±0.01a	0.51±0.06a	0.34±0.01e	0.78±0.02a	0.52±0.01d	0.78±0.01ab	0.66±0.06b	0.73±0.03b	0.76±0.03b	0.79±0.00abc	0.78±0.01b	0.79±0.01a

Values are presented as the mean ± standard deviation. Letters represent the significance of differences.

4. Discussion

Root rot is one of the main reasons for the decrease in *L. barbarum* yield, and *Fusarium* species are the main causative pathogens [38]. The root rot pathogens of *L. barbarum* mainly damage its rhizome, and diseased plants exhibit symptoms including root rot, leaf etiolation, wilting, and stunted growth, resulting in reduced water and nutrient transport and sometimes plant death [52]. The yield and quality of Gouqi berry decrease, causing serious economic losses. Nuomuhong Farm in Qinghai Province is one of the main *L. barbarum*–producing areas. The large-scale cultivation of *L. barbarum* has brought huge economic benefits. However, root rot is becoming increasingly serious in *L. barbarum*. To effectively control root rot in *L. barbarum*, it is necessary to identify the pathogens causing this disease.

Fusarium species are the most widely distributed fungi, and they are connected to the environment, plants, and insects [10]. Compound infection and toxin secretion by *Fusarium* cause many diseases, reducing yield and quality and economic benefits. In this study, 36 root samples were collected from 12 locations on Nuomuhong Farm, Qinghai Province, China, and 125 isolates were confirmed as pathogens based on Koch's postulates. The pathogenic isolates showed differences in colony color and morphological characteristics of conidia. Molecular biology analyses revealed that these pathogens belonged to 12 species. Among the isolated pathogens, *F. equiseti, C. rosea,* and *M. bolleyi* were dominant. *Fusarium avenaceum, F. citri, F. incarnatum, F. culmorum, F. oxysporum,* and *F. tricinctum* were isolated less frequently. Additionally, *F. sambucinum, F. acuminatum,* and *F. solani* were common species. To our knowledge, this is the first report of *M. bolleyi*, *F. avenaceum*, and *F. citri* as pathogens causing root rot in *L. barbarum* in China.

Uwaremwe et al. confirmed the presence of *Fusarium* species, including *F. oxysporum*, *F. solani*, *F. tricinctum*, and *F. chlamydosporum*, and *A. alternata*, which are responsible for root rot disease, in Gouqi plants in Gansu and Ningxia provinces, China [53]. Bai et al. first reported root rot caused by *F. culmorum* and *F. equiseti* on *L. barbarum* in Qinghai Province, China [52]. Feng et al. found that fungi isolated from Gouqi roots in the Qaidam Basin, China, were mainly *Fusarium* species, including *F.*

 doi:10.20944/preprints202509.2297.v1

lichenicola, *F. oxysporum*, *F. redolens*, and *F. solani*; *Plectosphaerella plurivora*; and *Ple. cucumerina*. *Mortierella alpina*, *Mucor hiemalis*, *Penicillium janthinellum*, *Verticillium nonalfalfae*, *C. rosea*, and *Pen. simplicissimum* were also identified [54]. Compared with these studies, in Qinghai, the composition of pathogenic fungi causing root rot on Gouqi differed. In this study, we found 12 species of pathogenic fungi, but *F. chlamydosporum*, *A. alternata*, *Plectosphaerella plurivora*, *Mortierella alpina*, and *P. cucumerina* were not found. We also identified *F. oxysporum*, *F. solani*, *F. tricinctum*, *F. culmorum*, *F. equiseti*, and *C. rosea*. This could have occurred because of regional differences and different planting years.

Pathogenic fungi infect the roots and rhizomes of *L. barbarum*, and root rot occurs from the seedling stage to the mature plant stage. In this study, the pathogenicity of 125 isolates was tested, and they could infect 1-year-old *L. barbarum* seedlings, as shown using scratching and root-irrigation inoculation techniques. *Fusarium* also affects other medicinal plants, such as *Angelica* [*55*] and *A. membranaceus* var. *mongholicus* [*56*], and leads to root rot and wilt in several important economic crops, including *Cucumis melo* [57], *C. sativus* [58] and *Solanum lycopersicum* [59]. Other plants, such as *Codonopsis pilosula* and *Zea mays*, also suffer from root and stem rot due to this pathogen. Furthermore, *Fusarium* causes needle blight in coniferous trees, such as *Pinus thunbergii* [60], and damping-off disease in *P. pinea* [*61*]. It also secretes toxins that contaminate fruit, reducing their shelf life. Common toxins produced by *Fusarium* include trichothecenes, zearalenones, fumonisins, beauvericin, and enniatins, all of which pose health risks to plants, livestock, and humans [62,63]. Efforts to control *Fusarium* in China primarily focus on selecting biocontrol microorganisms, including *Metarhizium robertsii* [*64*], *fluorescent Pseudomonas* [*65*], and *Trichoderma harzianum* [*66*], which have shown a control effect against root rot.

Morphological characteristics of pathogenic fungi from different hosts or different ecological regions vary to some extent. Research on the biological characteristics of plant pathogens lays the foundation for determining the occurrence patterns of diseases and formulating prevention and control measures. Therefore, the biological characteristics, including the optimal pH, temperature, and carbon and nitrogen sources, were also determined. Li et al. found that optimum growth conditions for *F. oxysporum*, causing black rot in *Gastrodia elata*, were as follows: pH 9, 28°C, fructose as a carbon source, and beef extract as a nitrogen source. The strain died after 40 min of treatment at 60°C [67]. Here, the optimum carbon source for *F. oxysporum* were sucrose, dextrin, soluble starch, and fructose, etc. The optimum nitrogen sources were beef extract, peptone, and yeast powder. The lethal temperature was 65°C, and the best pH was 10. The lethal temperature, and best pH differed from those reported by Li et al. [67]. According to Li et al., the optimum growth conditions for *F. solani*, causing black rot in *Gastrodia elata*, were as follows: pH 7, 30°C, mannitol as a carbon source, sodium nitrate as a nitrogen source, and PDA medium as a base medium. The strain died after 40 min of treatment at 65°C [67]. In this study, the optimum culture medium for *F. solani* was PDA, and the lethal temperature was 65°C. A pH of 10, a carbon source of mannitol, and a nitrogen source of sodium nitrate were optimal. Therefore, the results for *F. solani* are similar to those found by Li et al. [67]. Nikitin et al. found that *F. acuminatum* and *F. culmorum* were mostly identified in temperate climates and did not develop at temperatures above 25°C [68]. Li et al. found that *F. sambucinum* and *F. culmorum*, causing potato dry rot, were sensitive to temperature and pH. *Fusarium sambucinum* showed favorable growth on the glucose-based culture, while *F. culmorum* preferred the sucrose-based culture [69]. Here, the lethal temperature of *F. acuminatum* was 50°C, with the lethal temperature for *F. culmorum* was 50°C, and the best carbon source were sucrose, glucose, dextrin, and soluble starch. The biological characteristics of *F. acuminatum* and *F. culmorum* differed from those observed by Li et al. [69] and Nikitin et al. [68]. These differences in the biological characteristics might be related to the source, hosts, and environment of the isolates.

5. Conclusions

This study has provided preliminary insights into the fungal species responsible for root rot in *L. barbarum* at Nuomuhong Farm in Qinghai Province, China. Following Koch's postulates, 12

 doi:10.20944/preprints202509.2297.v1

pathogen species were identified to cause root rot in *L. barbarum*. The dominant pathogens included *F. equiseti*, *C. rosea*, and *M. bolleyi*. This research marks the first report of *M. bolleyi*, *F. avenaceum*, and *F. citri* as pathogens causing *L. barbarum* root rot in China. The lethal temperatures for these 12 pathogen species generally exceeded 50°C. The best media for the 12 pathogens were PDA, CM, and CLA. The optimum carbon sources were sucrose, dextrin and soluble starch, and the optimum nitrogen sources were beef extract, peptone, and yeast extract. These results establish a foundation for the comprehensive prevention and control of Gouqi root rot. Future studies should focus on the screening and development of control agents for these 12 pathogenic fungal species.

Supplementary Materials: The following supporting information can be downloaded at the website of this paper posted on Preprints.org. **Figure S1.** Maximum parsimony tree of root rot pathogens from *L. barbarum* inferred from rDNA-ITS sequences. The tree length is 3561. The CI, RI, and RC index were 0.537, 0.950, and 0.510, respectively. **Figure S2.** Maximum parsimony tree of root rot pathogens from *L. barbarum* inferred from *TEF-1α* gene sequences. The tree length is 3871. The CI, RI, and RC index were 0.582, 0.952, and 0.554, respectively. **Figure S3.** Maximum parsimony tree of root rot pathogens from *L.* barbarum inferred from *RPB2* gene sequences. The tree length is 7092. The CI, RI, and RC index were 0.594, 0.935, and 0.555, respectively. **Figure S4.** Effects of different media on the pathogen growth rate. **Figure S5.** Effects of different temperatures on the pathogen growth rate. **Figure S6.** Effects of different pH values on the pathogen growth rate. **Figure S7.** Effects of different carbon sources on the pathogen growth rate. **Figure S8.** Effects of different nitrogen sources on the pathogen growth rate.

Author Contributions: Writing this paper, Yongbao Zhao; Designed the experiments, Hexing Qi; Performed the experiments, Yongbao Zhao and Linshan Wang and Lijie Liu, Hexing Qi; Analyzed the data, Yongbao Zhao and Kaifu Zheng and Chengwen Zheng and Hexing Qi. All authors have read and agreed to the published version of the manuscript.

Funding: This research was funded by the Zhejiang Province Key Research and Development Program, grant number 2023C04023.

Data Availability Statement: The original contributions presented in this study are included in the article/Supplementary Material. Further inquiries can be directed to the corresponding author.

Institutional Review Board Statement: This study not involving humans or animals.

Conflicts of Interest: We declare that no conflict of interest exists.

References

1. Wetters, S.; Horn, T.; Nick, P. Goji Who? Morphological and DNA Based Authentication of a "Superfood". Front Plant Sci **2018**, 9, 1859. [CrossRef][PubMed]
2. Mocan, A.; Vlase, L.; Vodnar, D.C.; Bischin, C.; Hanganu, D.; Gheldiu, A.-M.; Oprean, R.; Silaghi-Dumitrescu, R.; Crișan, G. Polyphenolic Content, Antioxidant and Antimicrobial Activities of *Lycium barbarum* L. and *Lycium chinense* Mill. Leaves. Molecules **2014**, 19, 10056-10073. [CrossRef][PubMed]
3. Yao, R.; Heinrich, M.; Weckerle, C.S. The genus *Lycium* as food and medicine: A botanical, ethnobotanical and historical review. J Ethnopharmacol **2018**, 212, 50-66. [CrossRef][PubMed]
4. Burke, D.S.; Smidt, C.R.; Vuong, L.T. Momordica cochinchinensis, Rosa, roxburghii, wolfberry, and sea buckthorn-highly nutritional fruits supported by tradition and science. Curr Top Nutraceut R **2005**, 3(4), 259. [CrossRef]
5. Han, Y.; Zhou, Y.; Shan, T.; Li, W.; Liu, H. Immunomodulatory Effect of *Lycium barbarum* Polysaccharides against Liver Fibrosis Based on the Intelligent Medical Internet of Things. J Healthc Eng **2022**, 2022, 6280265. [CrossRef][PubMed]
6. Luo, Q.; Cai, Y.; Yan, J.; Sun, M.; Corke, H. Hypoglycemic and hypolipidemic effects and antioxidant activity of fruit extracts from *Lycium barbarum*. Life Sci **2004**, 76(2), 137-149. [CrossRef][PubMed]
7. Potterat, O. Goji (*Lycium barbarum* and *L. chinense*), Phytochemistry, pharmacology and safety in the perspective of traditional uses and recent popularity. Planta Med **2010**, 76(1), 7-19. [CrossRef][PubMed]

 doi:10.20944/preprints202509.2297.v1

8. Liang, X.; An, W.; Li, Y.; Qin, X.; Zhao, J.; Su, S. Effects of different nitrogen application rates and picking batches on the nutritional components of *Lycium barbarum* L. fruits. Front Plant Sci **2024,** 15, 355832. [CrossRef][PubMed]
9. Zhao, J.; Li, H.; Yin, Y.; An, W.; Qin, X.; Wang, Y.; Fan, Y. Li, Y.; Cao, Y. Fruit ripening in *Lycium barbarum* and *Lycium ruthenicum* is associated with distinct gene expression patterns. Febs Open Bi **2020,** 10(8), 1550-1567. [CrossRef][PubMed]
10. Gnaim, R.; Ledesma-Amaro, R. Synthetic biology of *Fusarium* for the sustainable production of valuable bioproducts. Biotechnol Adv **2025**, 108579. [CrossRef][PubMed]
11. Summerell, B.A. Resolving *Fusarium*, Current status of the genus. Annual review of phytopathol **2019**, 57(1), 323-339. [CrossRef]
12. Doshi, P.; Šerá, B. Role of Non-Thermal Plasma in *Fusarium* Inactivation and Mycotoxin Decontamination. Plants **2023**, 12, 627. [CrossRef][PubMed]
13. Zheng, J.; Wang, L.; Hou, W.; Han, Y. *Fusarium oxysporum* Associated with Fusarium Wilt on *Pennisetum sinese* in China. Pathogens **2022**,11(9), 999-999. [CrossRef][PubMed]
14. Khairullina, A.; Micic, N.; Jørgensen, H.J.L.; Bjarnholt, N.; Bülow, L.; Collinge, D.B.; Jensen, B. Biocontrol Effect of *Clonostachys rosea* on *Fusarium graminearum* Infection and Mycotoxin Detoxification in Oat (*Avena sativa*). Plants **2023**, 12, 500. [CrossRef][PubMed]
15. Thenuwara, G.; Akhtar, P.; Javed, B.; Singh, B.; Byrne, H.J.; Tian, F. Recent Advancements in Lateral Flow Assays for Food Mycotoxin Detection: A Review of Nanoparticle-Based Methods and Innovations. Toxins **2025**, 17, 348. [CrossRef][PubMed]
16. Ren, X.; Fan, L.; Li, G.; Lyagin, I.V.; Zhang, B.; Ning, M.; Yan, M.; Gao, J.; Wang, F.; Guo, C.; et al. Interaction of *Trichoderma* Species with *Fusarium graminearum* Growth and Its *Trichothecene* Biosynthesis as Further Contribution in Selection of Potential Biocontrol Agents. J. Fungi **2025**, 11, 521. [CrossRef]
17. Dean, R.; Van Kan, J.A.; Pretorius, Z.A.; Hammond-Kosack, K.E.; Di Pietro, A.; Spanu, P.D.; Rudd, J.J.; Dickman, M.; Kahmann, R.; Ellis, J.; Foster, G.D. The Top 10 fungal pathogens in molecular plant pathology. Mol Plant Pathol **2012**, 13(4), 414-30. [CrossRef][PubMed]
18. Lal, D.; Dev, D.; Kumari, S.; Pandey, S.; Aparna; Sharma, N.; Nandni, S.; Jha, R.K.; Singh, A. Fusarium wilt pandemic, current understanding and molecular perspectives. Funct Integr Genomic **2024**, 24(2), 41. [CrossRef][PubMed]
19. Munhoz, T.; Vargas, J.; Teixeira, L.; Staver, C.; Dita, M. *Fusarium* Tropical Race 4 in Latin America and the Caribbean, status and global research advances towards disease management. Front Plant Sci **2024**, 15, 1397617. [CrossRef][PubMed]
20. Szabo-Hever, A.; Sharma, J.S.; Faris, J.D.; Zhong, S.; Friesen, T.L.; Fiedler, J.D.; Green, A.J.; Bai, G.; Elias, E.M.; Xu, S.S. Identification and mapping of quantitative trait loci for Fusarium head blight resistance in a synthetic hexaploid × hard red spring wheat population. Plant Genome **2025,** 18(3), e70073. [CrossRef][PubMed]
21. Chen, S.Y.; Lai, M.H.; Tung, C.W.; Wu, D.H.; Chang, F.Y.; Lin, T.C.; Chung, C.L. Genome-wide association mapping of gene loci affecting disease resistance in the rice-*Fusarium fujikuroi* pathosystem. Rice (N Y) **2019**, 12(1), 85. [CrossRef][PubMed]
22. Xie, F.; Sun, Y.; Zhang, H.; Cui, J.; Wang, Q.; Gao, X. ZmBAK1 confers maize resistance to Gibberella stalk rot caused by *Fusarium graminearum* via activating PAMP-triggered immunity. Plant Signal Behav. **2025**, 20(1), 2502739. [CrossRef][PubMed]
23. Karlsson, I.; Persson, P.; Friberg, H. Fusarium Head Blight From a Microbiome Perspective. Front Microblol **2021**, 12, 628373-628373. [CrossRef][PubMed]
24. Pašakinskienė, I.; Stakelienė, V.; Matijošiūtė, S.; Martūnas, J. Diversity of Endophytic Fungi and Bacteria Inhabiting the Roots of the Woodland Grass, *Festuca gigantea* (Poaceae). Diversity **2024**, 16, 453. [CrossRef]
25. Matušinsky, P.; Florová, V.; Sedláková, B.; Mlčoch, P.; Bleša, D. Colonization dynamic and distribution of the endophytic fungus *Microdochium bolleyi* in plants measured by qPCR. PLoS One **2024**, 19(1), e0297633. [CrossRef][PubMed]
26. Ünal, F. Phylogenetic analysis of *Microdochium* spp. associated with turfgrass and their pathogenicity in cereals. Peer J **2024**,12, e16837-e16837. [CrossRef][PubMed]

 doi:10.20944/preprints202509.2297.v1

27. Sung, K.H.; Wan, G.K.; Hyo, W.C.; Lee, S.Y. Identification of *Microdochium bolleyi* associated with basal rot of creeping bent grass in Korea. Mycobiology **2008**, 36(2), 77-80. [CrossRef][PubMed]
28. Black, D.L.R.; Brown, A. E. *Microdochium bolleyi* associated with root rot of flax. Plant Pathol **1986**, 35(4), 592-659. [CrossRef]
29. Liu, J.; Sun, S.; Chen, K.; Gao, S.; Chen, D.; Zhang, Y.; Hu, C. Discerning promotion mechanisms of fungi *Clonostachys rosea* on growth of freshwater microalga Chlorella sp. by non-contact culture. Algal Research **2025**, 86103967-103967. [CrossRef]
30. Shravani, V.; Iruthayasamy, J.; Nallusamy, S.; Govindasamy, J.; Eswaran, K.; Annaiyan, S. Unveiling *Clonostachys rosea* bioactives, Investigating antifungal potential against *Fusarium oxysporum* through in vitro and in silico studies. Research Square **2024**. [CrossRef]
31. Petrucci, A.; Cesarini, M.; Vicente, I.; Merani, L.; Jensen, B.; Collinge, D.B.; Sarrocco, S. Exploring the syner[Error! Reference source not found.]gistic potential of *Trichoderma gamsii* T6085 and *Clonostachys rosea* IK726 for biological control of Fusarium head blight in wheat. Microbiol Res **2025**, 296128152. [CrossRef][PubMed]
32. Bienapfl, J. C.; Floyd, C. M.; Percich, J. A.; Malvick, D. K. (2012). First report of *Clonostachys rosea* causing root rot of soybean in the United States. Plant Dis **2012**, 96(11), 1700-1700. [CrossRef][PubMed]
33. Zhao, J.; Xu, X.; Xu, X.; Guo, L.; Wang, X.; Xiang, W.; Zhao, J. Identification and pathogenicity of *Clonostachys* spp. and its co-inoculation with *Fusarium* species on soybean root. Plant Pathol **2024**, 73(7), 1801-1811. [CrossRef]
34. Li, Y.L.; Sun, Z.M.; Li, S.K.; Zhao, X.S.; Abiodun, O.; Han; Z. M. First report of root rot caused by *Clonostachys rosea* on *Xanthoceras sorbifolium* in China. Plant Dis **2024**, 108(3), 798. [CrossRef]
35. Bienapfl, J.C.; Floyd, C.M.; Percich, J.A.; Malvick, D.K. First report of *Clonostachys rosea* Causing Root Rot of Soybean in the United States. Plant Dis **2012**, 96(11), 1700. [CrossRef][PubMed]
36. Díaz, R.; Chávez, E.C.; Delgado-Ortiz, J. C.; Velazquez Guerrero, J. J.; Roque, A.; Ochoa, Y.M. First report of *Clonostachys rosea* causing root rot on garlic in Mexico. Plant Dis **2022**, 106(11), 3000. [CrossRef]
37. Qi, H.; Duan, X.; Xu W.; Zhou, Y.; Ma, H.; Ma, W.; Ma, G. First report disease of *Clonostachys rosea* causing root rot on *Astragalus membranaceus* in China. Plant Dis **2022**, 106(6), 1752. [CrossRef]
38. Li, N.; Chen, W.; Wang, B.; Zhang, C.; Wang, Y.; Li, R.; Yan, Y.; He, J. Arbuscular mycorrhizal fungi improve the disease resistance of *Lycium barbarum* to root rot by activating phenylpropane metabolism. Front Plant Sci **2024**, 15, 1459651. [CrossRef][PubMed]
39. Xu, C.Y.; Gao, H.H.; Han, Q.; Jia, C.B.; Swingle, B.; Gao, M.; Su, J.Y. First report of *Fusarium redolens* causing root rot of Goji berry cv. 'Ningqi-7' in China. J Phytopathol **2024**, 172(2), e13278. [CrossRef]
40. Zhang, T.; Zhang, Z.; Li, Y.; He, K. The Effects of Saline Stress on the Growth of Two Shrub Species in the Qaidam Basin of Northwestern China. Sustainability-basel **2019**, 11, 828. [CrossRef]
41. Chen, X. L.; Yang, J.; Peng, Y. L. Large-scale insertional mutagenesis in Magnaporthe oryzae by Agrobacterium tumefaciens-mediated transformation. Methods in molecular biology **2011**, 722, 213–224. [CrossRef][PubMed]
42. Leslie, J.F.; Summerell, B.A. The Fusarium laboratory manual. John Wiley & Sons **2008**. [CrossRef]
43. Xu, J. R.; Hamer, J. E. MAP kinase and cAMP signaling regulate infection structure formation and pathogenic growth in the rice blast fungus Magnaporthe grisea. Genes development **1996**, 10(21), 2696–2706. [CrossRef][PubMed]
44. Utama, G.L.; Lestari, W.D.; Kayaputri, I.L.; Balia, R.L. Balia. Indigenous yeast with cellulose-degrading activity in napa cabbage (*Brassica pekinensis* L.) waste, Characterisation and species identification. Foods and Raw Materials **2019**, 321-328. [Crossref]
45. White, T. J.; Bruns, T.; Lee, S. J. W. T.; Taylor, J. Amplification and direct sequencing of fungal ribosomal RNA genes for phylogenetics. PCR protocols, a guide to methods and applications **1990**, 18(1), 315-322. [CrossRef]
46. Wong, J.Y.; Jeffries, P. Diversity of pathogenic Fusarium populations associated with asparagus roots in decline soils in Spain and the UK. Plant Pathol **2006**, 55(3), 331-342. [CrossRef]
47. Bueno, C.J.; Fischer, I.H.; Rosa D.D.; Firmino, A.C.; Harakava, R.; Oliveira C.M.G.; Furtado, E.L. *Fusarium solani* F. sp. *Passiflorae*: a new forma specialis causing collar rot in yellow passion fruit. Plant Pathol **2014**, 63(2), 382-389. [CrossRef]

 doi:10.20944/preprints202509.2297.v1

48. Zhao, J.; Huang, M. Characterization and In Vitro Fungicide Sensitivity of Two *Fusarium* spp. Associated with Stem Rot of Dragon Fruit in Guizhou; China. J Fungi **2023**, 9(12), 1178. [CrossRef][PubMed]
49. Swofford, D.L. PAUP* [Phylogenetic Analysis Using Parsimony (*and Other Methods)], Version 4. Sinauer Associates **2003**, Sunderland, MA.[CrossRef]
50. Zhao, X.; Gao, C.; Zhang, X.; Du, M.; Wang J.; Wang, X.; Lu, B.; Chen, C.; Yang, L.; Zhang, Y. et al. Identification and biological characteristics of *Fusarium tobaccum* sp. nov.; a novel species causing tobacco root rot in Jilin Province; China. Microbiol Spectr **2024**, 12(12), e00925-24. [CrossRef][PubMed]
51. Yang, E.; Fan, L.; Yan, J.; Jiang, Y.; Doucette, C.; Fillmore, S.; Walker; B. Influence of culture media; pH and temperature on growth and bacteriocin production of bacteriocinogenic lactic acid bacteria. AMB express **2018**, 8, 1-14. [CrossRef][PubMed]
52. Bai, L.; Li, X.; Cao, Y.; Song, Z.; Ma, K.; Fan, Y.; Ma, M. *Fusarium culmorum* and *Fusarium equiseti* causing root rot disease on *Lycium barbarum* (goji berry) in China. Plant Dis **2020**, 104(11), 3066. [CrossRef]
53. Uwaremwe, C.; Yue, L.; Liu, Y.; Tian, Y.; Zhao, X.; Wang, Y.; Xie, Z.; Zhang, Y.; Cui, Z.; Wang, R. Molecular identification and pathogenicity of *Fusarium* and *Alternaria* species associated with root rot disease of wolfberry in Gansu and Ningxia provinces; China. Plant Pathol **2021**, 70(2), 397-406. [CrossRef]
54. Feng, Zhilin; Xiao, Y.; Li, N.; Gao, Q.; Wang J.; Chen, S.; Xing, R. Effects of root rot on microbial communities associated with goji berry (*Lycium barbarum*) in the Qaidam Basin; China European Journal of Plant Pathol **2023**,167, 853-866. [CrossRef]
55. Zhang, Z.; Zhang, W.; Wang, X.; Kou, Z.; Wang, Y.; Islam, R.; Zhang, J.Q.; Liu, L.; Xie, T.; Tian, Y.Q. Isolation and identification of antagonistic bacteria of *Angelica* root rot and their mechanism as biological control. Biological Control **2023**, 177, 105120. [CrossRef]
56. Qi, H.; Qi, X.; Xu, W.; An, Z.; Fan, T. First Report of Root Rot Caused by *Fusarium avenaceum* and *Fusarium flocciferum* on *Astragalus membranaceus* var. *mongholicus* in China. J Phytopathol **2024**, 172(5), e13397. [CrossRef]
57. Sabahi, F.; Banihashemi, Z.; Mirtalebi, M.; Rep, M.; Cacciola, S.O. Molecular Variability of the *Fusarium solani* Species Complex Associated with Fusarium Wilt of Melon in Iran. J. Fungi **2023**, 9, 486. [CrossRef][PubMed]
58. Williams, H. Root and stem rot of cucumber caused by *Fusarium oxysporum* f. sp. *radicis-cucumerinum* f. sp. nov. Plant Dis **1996**, 80(3), 313. [CrossRef]
59. Ye, Q.; Wang, R.; Ruan, M.; Yao, Z.; Cheng, Y.; Wan, H.; Li, Z.; Yang, Y.; Zhou, G. Genetic diversity and identification of wilt and root rot pathogens of tomato in China. Plant Dis **2020**, 104(6), 1715-1724. [CrossRef][PubMed]
60. Ding, X.L.; Lin, S.X.; Zhao, R.W.; Ye, J.R. First report of needle blight on *Pinus thunbergii* Caused by *Fusarium proliferatum* in China. Plant Dis **2022**, 106(11), 2989. [CrossRef]
61. Tahat, M.M.; Aldakil, H.A.; Alananbeh, K.M. First report of damping off disease caused by *Fusarium oxysporum* on *Pinus pinea* in Jordan. Plant Dis **2021**, 105(12), 4153. [CrossRef]
62. Desjardins, A.E.; Proctor, R.H. Molecular biology of *Fusarium mycotoxins*. International journal of food microbiol **2007**, 119(1-2), 47-50. [CrossRef][PubMed]
63. Wang, Q.; Xu, L. Beauvericin, a Bioactive Compound Produced by Fungi: A Short Review. Molecules **2012**, 17, 2367-2377. [CrossRef][PubMed]
64. He, J.; Zhang, X.; Wang, Q.; Li, N.; Ding, D.; Wang, B. Optimization of the fermentation conditions of Metarhizium robertsii and its biological control of wolfberry root rot disease. Microorganisms **2023**, 11(10), 2380. [CrossRef][PubMed]
65. Lemanceau, P.; Alabouvette, C. Biological control of fusarium diseases by fluorescent Pseudomonas and non-pathogenic *Fusarium*. Crop protection **1991**, 10(4), 279-286.
66. Sivan, A; Chet, I. Biological control of *Fusarium* spp. in cotton; wheat and muskmelon by *Trichoderma harzianum*. J. Phytopathol **1986,** 116(1), 39-47.
67. Li, J.; He, K.; Zhang, Q.; Wu, X.; Li, Z.; Pan, X.; Wang, Y.; Li, C.; Zhang, M. Draft Genome and Biological Characteristics of *Fusarium solani* and *Fusarium oxysporum* Causing Black Rot in *Gastrodia elata*. Int. J. Mol. Sci **2023,** 24, 4545.

 doi:10.20944/preprints202509.2297.v1

68. Nikitin, D.A.; Ivanova, E.A.; Semenov, M.V.; Zhelezova, A.D.; Ksenofontova, N.A.; Tkhakakhova, A.K.; Kholodov, V.A. Diversity, Ecological Characteristics and Identification of Some Problematic Phytopathogenic Fusarium in Soil: A Review. Diversity **2023**, 15, 49.
69. Li, F.; Jiang, X.; Sun, M.; Xu, H.; Shi, L.; Shan, W. Screening of culture conditions for pathogens of potato dry rot. Acta Agr Scand B-S P **2014,** 64(8), 694-699.